The Effect of Nanofibers on Liquid–Liquid Coalescence Filter Performance

C. Shin and G. G. Chase
Microscale Physiochemical Engineering Center, University of Akron, Akron OH 44325

D. H. Reneker
Maurice Morton Institute of Polymer Science, University of Akron, Akron OH 44325

DOI 10.1002/aic.10564
Published online August 10, 2005 in Wiley InterScience (www.interscience.wiley.com).

A number of factors influence the efficiency and the economics of the separation of dispersed liquid drops in an immiscible liquid–liquid mixture. One important factor that controls the performance of a filter medium in the separation is the fiber size. Electrospun polymer nanofibers have diameters in the nanometer range and are arbitrarily long. The experimental results in this work show that adding nanofibers to conventional micron-sized fibrous filter media improves the separation efficiency of the filter media but also increases the pressure drop. An optimum in the performance occurs (significant increase in efficiency with minimal increase in pressure drop) with the addition of about 1.6% by mass of 250 nm diameter nylon 6 nanofibers to 5 micron diameter glass fibers in the filters.
 AIChE J, 51: 3109–3113, 2005
Keywords: nanofibers, coalescence, filtration, filter media

Introduction

Glass-fiber filter media augmented with small amounts of nanofibers show improvement of separation efficiency. Filter media with equal amounts of nanofibers made of MPD-I [meta-aramid, poly(meta-phenyleneisophthalamide)], nylon 6, or polyacrylonitrile (PAN) were tested for liquid–liquid coalescence filtration in a previous article.[1] The aim of the study reported in this article is to present the effects of varying the amount of nylon 6 nanofiber added to the glass-fiber media on the pressure drop and the separation efficiency in liquid–liquid coalescence filter performance. The nanofibers are produced by electrospinning and have diameters typically in the range of 10–500 nm.[2-5]

The electrospinning process is driven by the electrical forces on free charges on the surface or inside of a polymeric liquid. When the free charges, generally ions, in the polymer solution move in response to the electric field, they quickly transfer a force to the polymer solution. When the electric field reaches a critical value at which the repulsive electric force between charges on the surface overcomes the surface tension force, a charged jet of the solution is ejected from the tip of a cone protruding from a liquid drop of the polymer. As the jet stretches and elongates in the air, the solvent evaporates, leaving behind a charged solid polymer fiber that lays itself randomly on a collecting metal screen. Thus, continuous fibers are produced to form a nonwoven fabric.[2,6] Nonwoven mats of electrospun fibers have a large surface area per unit mass and small pore sizes compared to those of commercial textiles, making them excellent materials for use in filtration applications.[7]

Water-in-oil emulsion separation is important to the petroleum and chemical industries to remove the dispersed liquid for safety, ecologic, and economic reasons. The coalescence filter is effective for separation of secondary dispersions, although dispersions of drops with diameters $< 100\ \mu$m can be difficult to separate. Fibrous filter media can provide high filtration efficiency with low pressure drop, depending on the flow rate, bed depth, fiber surface properties, fiber size, drop size, and fiber orientation.[8-21]

Correspondence concerning this article should be addressed to G. G. Chase at gchase@uakron.edu.

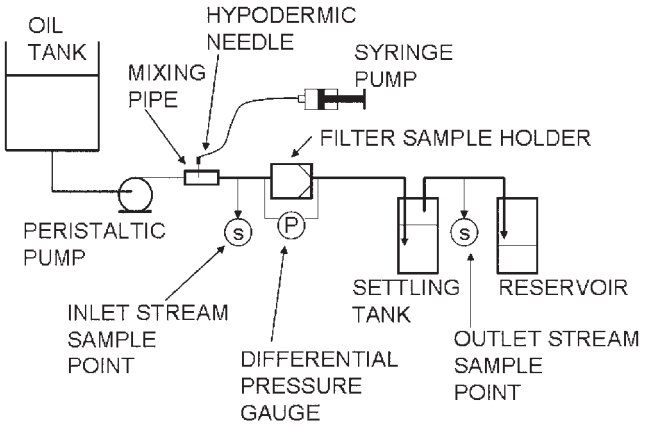

Figure 1. Experimental apparatus for filter testing.

Oil from the oil tank is pumped through a mixing pipe, through a filter sample holder, into a settling tank, and into a reservoir. Water droplets are dispersed into the oil by injection from a syringe into the mixing pipe. Emulsion samples are removed from the flow stream for drop size measurements at the sample points upstream (U) and downstream (D) of the filter. The latter is located between the settling tank and the reservoir.

Experimental Setup and Procedures

The experimental apparatus is shown in Figure 1. A mixture of water-in-oil was used in the experiments, in which deionized water droplets were dispersed in an oil phase having properties similar to those of diesel fuel (Viscor 1487™, specific gravity = 0.83; Rock Valley Oil and Chemical Company). The Viscor 1487 ™ is pumped from the oil tank by a peristaltic pump, at a constant flow rate, through a mixing pipe (where the water drops are mixed with the oil), through the filter sample and into a settling tank and a reservoir. The flow rate is controlled by selection of the tube diameter for the peristaltic pump. A flow rate of 100 mL/min was used in all experiments in this work.

The water-in-oil emulsion is produced in the mixing pipe. The mixing pipe is a Plexiglas® tube with a 1 mm inside diameter. The mixing pipe is inserted into the flexible tube between the pump and the filter sample. Water is pumped by a syringe pump (Model Sp101i, with flow ranges from 0.001 to 1.175 mL/min; World Precision Instruments, Sarasota, FL) through a hypodermic needle into the middle of the mixing pipe through which the oil flows. A very fine water-in-oil emulsion is produced at the outlet of the hypodermic needle, arising from the shear force created by the flowing oil phase, in which 99.8% of water droplets are <30 microns,. The concentration of water and size of the droplets are controlled by adjusting the water flow rate using the syringe pump and the velocity of the oil past the tip of the needle.

The water droplets produced in the mixing pipe do not settle out of the oil for a reasonable length of time. The water droplets in the oil come into contact with each other in the filter medium and form larger coalesced droplets of water that are carried downstream to the settling tank. The larger drops are easily separated from the oil in the settling tank. Smaller drops that do not settle out by gravity are carried into the reservoir tank.

Samples of the water-in-oil emulsion are taken at intervals of 10 to 25 min from the flow system at sample points upstream of the filter (the inlet stream) and downstream of the settling tank as shown in Figure 1 (the outlet stream). The size distributions of water droplets in the emulsion samples are measured with a particle size analyzer (Hyac Royco BR8 particle counter, eight channels with sizes from 1 to 150 microns). Some of the coalesced drops exiting the filter media are too large for the BR8 to measure. Because of this the measurement point for the outlet stream was positioned downstream of the settling tank. The measured performance is a combination of the filter and the settling tank.

Separation performance can be characterized on a total mass basis, but the mass basis is biased to larger drop sizes. To determine how the separation efficiency varies with droplet size, the separation efficiency of droplets of size x is defined as

$$e = \frac{\text{Number of drops of size } x \text{ removed}}{\text{Number of drops of size } x \text{ in the inlet}} \tag{1}$$

This equation is rewritten in terms of the number of drops of size x measured in the outlet stream as

$$e(x) = 1 - \frac{n_O(x)}{n_I(x)} \tag{2}$$

where $n_O(x)$ is the number count of drops of average size x for a size range Δx in the outlet stream and $n_I(x)$ is the number count of drops of the same average size and size range in the inlet stream.

The filter media samples used in the experiments are formed from glass fibers, nanofibers, and a binder (Carboset 560™, BF Goodrich) by vacuum molding an aqueous slurry of fibers and binder. Sulfuric acid is added to the slurry to adjust the pH in the range of 2.0 to 2.5 to disperse the glass fibers. The nanofibers are electrospun directly into the surface of the aqueous slurry of glass fibers and binder solution and the mixture is agitated using injected air.[25]

Figure 2 shows the apparatus used for electrospinning the nanofibers. A nylon-6 solution is prepared by dissolving 16 wt % nylon-6 by mass in 84 wt % formic acid.[1] The polymer

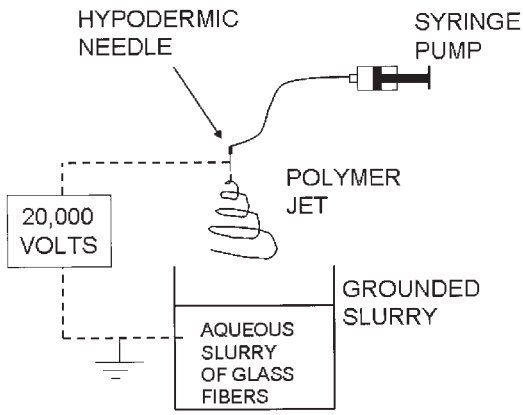

Figure 2. Experimental apparatus of electrospinning.

The polymer is pumped through the hypodermic needle. The needle is charged to 20,000 volts. The polymer jets from the needle, elongates into nanofibers, and collects on the surface of the slurry of glass fibers.

Table 1. Masses of Fibers in the Filter Media and Measured Separation Efficiencies

Filter	Glass-Fiber Mass (g)	Binder* Mass (g)	Nanofiber Mass (g)	Total Filter Sample Mass (g)
A	0.500	0.325	0	0.825
B	0.500	0.334	0.007	0.841
C	0.500	0.361	0.014	0.875
D	0.500	0.359	0.020	0.879
E	0.500	0.374	0.039	0.913

*Calculated by subtracting the fiber amounts from the total filter mass.

solution is loaded into the syringe and pumped through a needle suspended about 20 cm above the aqueous slurry surface. The syringe pump is set at a rate of 4.1 microliters per minute and the needle is charged to 20,000 to 25,000 volts to spin the polymer nanofibers.

Results and Discussion

The aim of this research is to investigate the effects of adding varying amounts of polymer nanofibers to glass-fiber media on filter media performance. Five filters labeled A through E, as listed in Table 1, were made by electrospinning varying amounts of nylon-6 nanofibers in each filter sample. Table 1 lists the masses of each fiber type, the mass of binder added to the filter to glue the fibers together, and the total mass of each filter sample. Each sample was made in triplicate and the average values of the three samples are listed in the table. The nanofibers spun from the apparatus described in Figure 2 had diameters varying from 200 to 300 nm, with an average diameter of about 250 nm (Figure 3). SEM images such as Figure 3 show that nanofibers appear as a single fiber intermingled with the larger glass fibers. The nanofibers crisscross over the void space between the larger glass fibers and are supported by the glass fibers. The glass fibers have diameters varying from about 2 to about 7 microns, with an average diameter of about 5 microns and lengths varying from about 100 microns to 1 mm.

The steady-state number counts of particles for different bin sizes from the filtration experiments are shown in Figure 4. The

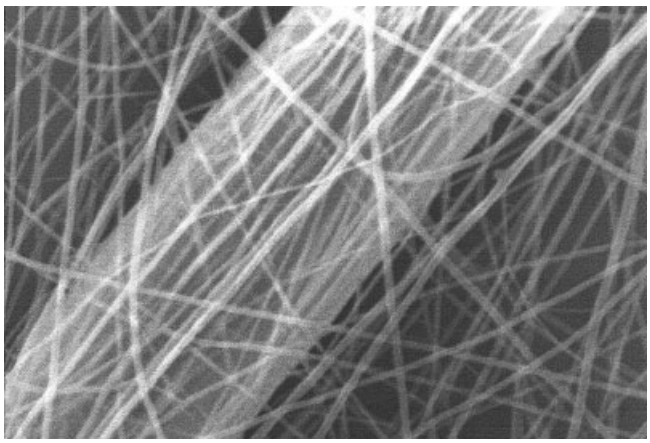

Figure 3. SEM image of a 5 micron diameter commercial glass fiber and 250 nanometer diameter electrospun nylon 6 polymer nanofibers.

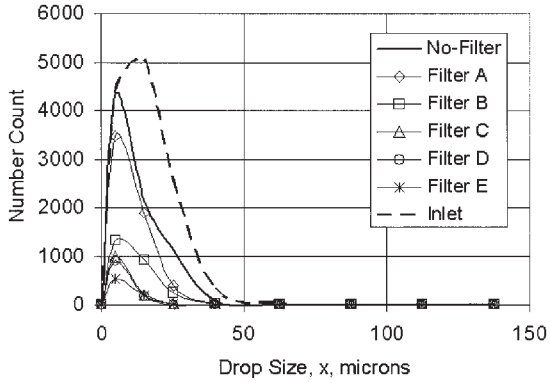

Figure 4. Steady-state drop size distributions measured in the inlet stream before the filter holder and in the outlet stream between the settling tank and the reservoir.

The curve marked as No Filter is the measured outlet distribution for when no filter is present in the filter holder. The curves marked Filter A through Filter E are the distributions for when the filters are tested in the holder.

drop size on the horizontal axis is the average drop size of the particular bin (the bin sizes in the BR8 are specified by the largest particle size in that particular bin). The size distribution marked as "Inlet" is the size distribution measured from the sample point upstream of the filter. The distribution marked as "No-Filter" was measured at the outlet stream sample point between the settling tank and the reservoir when no filter was in the holder. The difference between the "Inlet" and "No-Filter" curves shows some of the particles are separated out by the settling tank even when there is no filter in the line. The distribution curves marked as "Filter A" through "Filter E" were similarly measured at the outlet stream sample point and are the steady-state downstream distributions when the filters are placed in the line. With filters in the line the downstream numbers of particle concentrations are significantly reduced. The design of the settling tank may influence these results; thus, the same settling tank was used for all experiments and these results are comparable between the experiments for relative performance.

Figure 5 shows the separation efficiency distributions. The system with no filter approaches 100% efficiency for drop sizes $>$ 125 microns. All of the filters approach 100% efficiency for sizes $>$ 100 microns. Filter A shows a separation efficiency of 67% for drop size of 125 microns, but this low efficiency is attributed to one drop detected in the outlet stream from Filter A, whereas the inlet stream contained three such drops.

In the 0 to 100 micron drop size range significant differences in performance are noted. Filter A performs better than No Filter; Filter B performs better than Filter A; and Filters C, D, and E all perform about the same, all better than Filter B.

The steady-state pressure drops across the filters are shown in Figure 6. The filters supplemented with nanofibers have a higher pressure drop than that of filters without nanofibers. The change in pressure drop with the addition of nanofibers is almost linear. Because Filters C, D, and E have similar high capture efficiencies then an optimum design is one that has the

least pressure drop among the filters with the highest capture efficiencies. This means that, of the filters tested here, Filter C with 0.014 g of nanofiber (about 1.6% of the filter mass) is the optimum design.

The pore sizes in the microfiber filters (no nanofibers) are typically the same order of magnitude as that of the fiber diameter (about 5 microns). Large droplets are easily captured by interception with multiple fibers and the efficiency for microfiber filters is high for the larger drops. A greater fraction of smaller drops near the pore size may pass through the pores without coalescing into larger drops. Thus the filter efficiency decreases for smaller droplet sizes.

Results of this study confirm that the addition of nanofibers improves the filter performance. The nanofibers crisscross over pore spaces, making the pore openings much smaller. Thus it is more difficult for smaller drops to pass through the pores without coalescing with other drops.

For the drop sizes considered herein the dominant mechanism of capture is by direct interception and inertial impaction with multiple fibers. Most of the droplets are larger than the pore openings, and thus the mechanism of single-fiber capture does not apply. The small diameter of the nanofiber allows us to reduce the pore sizes with the addition of only small amounts of nanofibers and yet maintain a high porosity.

Other mechanisms, such as surface wetting properties, may influence the coalescence performance. We consider the interception of the drops by the nanofibers to be more important in this work.

Conclusions

In this work, the effect of different amounts of polymer nanofibers added to the filter media is experimentally evaluated. The addition of nanofibers to glass-fiber filter media improves the capture efficiency, but also causes an increase in pressure drop. The experimental results show that an optimal amount of nanofiber enhances the capture efficiency but does not cause excessive pressure drop. For the materials tested herein 1.6% nanofiber by mass is optimal.

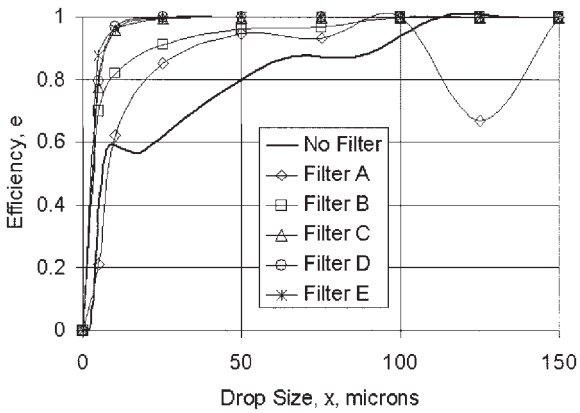

Figure 5. Separation efficiency by drop size.

Separation efficiencies (especially for the smaller drop sizes) increase with the nanofiber amount up to about 0.014 g of nanofiber. Filters of equal or greater than 0.014 grams of nanofiber performed at about the same efficiency.

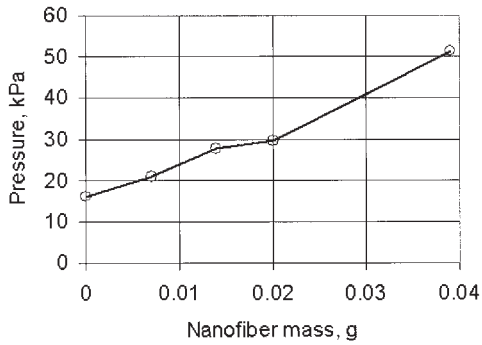

Figure 6. Pressure drop vs. the amount of nanofiber added to the glass-fiber filters.

Acknowledgments

This work was supported by Ahlstrom Paper Group, Donaldson Company, Fleetguard Inc., Hollingsworth and Vose, Parker Hannifin, and Produced Water Seminar. This work was also partially supported by National Science Foundation Grants CTS-0310429 and DMI-0403835.

Literature Cited

1. Shin C, Chase GG. Water-in-oil coalescence using glass fiber filters augmented with polymer nanofibers. *AIChE J.* 2004;50:343-350.
2. Reneker DH, Chun I. Nanometre diameter fibres of polymer, produced by electrospinning. *Nanotechnology.* 1996;7:216-223.
3. Reneker DH, Yarin AL, Fong H, Koombhongse S. Bending instability of electrically charged liquid jets of polymer solutions in electrospinning. *J Appl Phys.* 2000;87:4531-4547.
4. Shin YM, Hohman MM, Brenner MP, Rutledge GC. Electrospinning: A whipping fluid jet generates submicron polymer fibers. *Appl Phys Lett.* 2001;78:1149-1151.
5. Gibson P, Schreuder-Gibson H, Rivin D. Transport properties of porous membranes based on electrospun nanofibers. *Colloids Surf A.* 2001;187/188:469-481.
6. Doshi J, Reneker DH. Electrospinning process and applications of electrospun fibers. *J Electrostat.* 1995;35:151-160.
7. Deitzel JM, Kleinmeyer J, Harris D, Beck Tan NC. The effect of processing variables on the morphology of electrospun nanofibers and textiles. *Polymer.* 2001;42:261-272.
8. Sareen SS, Rose PM, Gudesen RC, Kintner RC. Coalescence in fibrous beds. *AIChE J.* 1966;12:1045-1050.
9. Fahim MA, Akbar AM. Removal of fine oily hazes from wastewater using deep fibrous bed coalescer. *J Environ Sci Health.* 1984;A19: 299-319.
10. Othman FM, Fahim MA, Jeffreys GV, Mumford GJ. Prediction of predominant mechanisms in the separation of secondary dispersion in a fibrous bed. *J Dispers Sci Technol.* 1988;9:91-113.
11. Šecerov Sokolovic RM, Sokolovic SM, Đ-Okovic BD. Effect of working conditions on bed coalescence of an oil-in-water emulsion using a polyurethane foam bed. *Ind Eng Chem Res.* 1997;36:4949-4953.
12. Moses SF, Ng KM. A visual study of the breakdown of emulsions in porous coalescers. *Chem Eng Sci.* 1985;40:2339-2350.
13. Hajra MG, Mehta K, Chase GG. Humidity, temperature, and polymer nanofibers on drop coalescence in glass fiber media. *Sep Purif Technol.* 2003;30:79-88.
14. Hazlett RN. Fibrous bed coalescence of water: Role of a sulfonate surfactant in the coalescence process. *Ind Eng Chem Fundam.* 1969; 8:633-640.
15. Hazlett RN. Fibrous bed coalescence of water: Steps in the coalescence process. *Ind Eng Chem Fundam.* 1969;8:625-632.
16. Akbar AM, Othman FM. Prediction of oil saturation in a fibrous bed coalescer from pressure drop data. *J Dispers Sci Technol.* 1989;10: 697-713.
17. Chase GG, Beniwal V, Venkataraman C. Measurement of uni-axial fiber angle in non-woven fibrous media. *Chem Eng Sci.* 2000;55:2151-2160.

18. Sherony DF, Kintner RC. Coalescence of an emulsion in fibrous bed: Part I. Theory. *Can J Chem Eng.* 1971;49:314-320.
19. Sherony DF, Kintner RC. Coalescence of an emulsion in fibrous bed: Part II. Experimental. *Can J Chem Eng.* 1971;49:321-325.
20. Spielman LA, Goren LG. Theory of coalescence by flow through porous media. *Ind Eng Chem Fundam.* 1972;11:66-72.
21. Chokdeepanich S. *Coalescence Filtration and Drainage Design*. PhD Dissertation. Akron, OH: The University of Akron; 2002.
22. Allen T. *Particle Size Measurement*. Vol. 1, 5th Edition. London, UK: Chapman & Hall; 1997.
23. Svarovsky L. *Solid–Liquid Separation*. 3rd Edition. London, UK: Butterworths; 1990.
24. Brown RC. *Air Filtration*: *An Integrated Approach to the Theory and Applications of Fibrous Filters*. New York, NY: Pergamon; 1993.
25. Chase GG, Reneker D, Rangarajan S, Mehta K. *Method and Apparatus of Mixing Fibers*. WO Patent No. 01/68228A1; 2001.

Manuscript received Feb. 20, 2004, and revision received Apr. 5, 2005.